Scientific Review – Engineering and Environmental Sciences (2019), 28 (4), 526–538
Sci. Rev. Eng. Env. Sci. (2019), 28 (4)
Przegląd Naukowy – Inżynieria i Kształtowanie Środowiska (2019), 28 (4), 526–538
Prz. Nauk. Inż. Kszt. Środ. (2019), 28 (4)
http://iks.pn.sggw.pl
DOI 10.22630/PNIKS.2019.28.4.48

Marek CHALECKI, Jacek JAWORSKI, Olga SZLACHETKA

Faculty of Civil and Environmental Engineering, Warsaw University of Life Sciences – SGGW

First natural frequency of multi-segment floor joists with variable cross section*

Key words: floor joist, first natural frequency, Rayleigh method

Introduction

Application of bar elements with variable cross sections provides an opportunity to reduce mass of mechanical systems, thus it is often employed. One of important aspects of the design of building constructions is calculation of the first natural frequency – both of the whole construction and of its separate elements – which is required by law. The papers focused on the determination of forms and frequencies of natural vibrations usually concern elements (beams, bars) having the shape of truncated cone, wedge and multiple-stepped beam. The mode shapes and natural frequencies can be determined from the Euler–Bernoulli differential equation of beam deflection. It can be solved with the Bessel functions of the second kind what, for truncated cone and truncated wedge beams, was presented by Conway and Dubil (1965). Ece, Aydogdu and Taskin (2007) assumed an exponential variability of beam width what enabled to solve the equation of beam vibrations in an exact way, using the method of separation of variables. Naguleswaran (1994) obtained an exact solution for double-tapered beam using the Frobenius method and submitting the tabulated results for various types of beams. For beams of bilinearly varying thickness, Laura, Gutierrez and Rossi (1995) compared values of the dimensionless fundamental frequency obtained by means of three methods: the optimized Rayleigh–Ritz method, the finite element approach and the differential quadrature technique – reaching very good agreement between the Rayleigh–Ritz method and FEM. The multi-segment (stair-shaped) beams were analysed also by Naguleswaran (2002, 2004). Mao (2011) compared the dimensionless frequency from the Naguleswaran's paper (2002) to

*Due to complexity of the article text was formatted in one-colunm page style.

his own results obtained by use of the Adomian decomposition method for two-step beam with constant thickness and step-varying width as well as for three step beam with constant width and varying height – reaching the "excellent" agreement. Duan and Wang (2013) studied free vibrations for multiple-stepped beams using the modified discrete singular convolution. Vaz and de Lima Junior (2014) calculated with numerical methods the mode shape of multiple-stepped beams with changes in cross section and compared it with experimental results. Tan, Wang and Jiao (2016) also considered natural (transversal) vibrations of multi-segment beams, obtaining exact results by using transfer matrix method, the exact general solutions of a one-step beam and iterative method.

The first frequency of natural (transversal) vibrations of bars with variable cross section can be estimated using the Rayleigh's method consisting in comparison of the potential (elastic) and kinetic energy of a vibrating beam. The basic assumption (and obvious simplification) of this method is that the first mode shape is the same as beam deflection due to constant static loads. Making this assumption, Jaworski, Szlachetka and Aguilera-Cortés (2015) analysed cantilever bars with variable cross sections – error of obtained results is small, thus this method can be applied in practice. Such approach was applied to analyse of vibrations of a solid and hollow truncated cone (conical pipe) with generatrices having the shape of straight line and concave parabola (Jaworski & Szlachetka, 2017) as well as convex parabola (Szlachetka, Jaworski & Chalecki, 2017). According to these papers, differences between the results obtained by means of this approach and those obtained with FEM do not exceed 3%.

Using the Rayleigh's method for beams with variable cross section with assumption that the first mode shape is the same as a shape of the axis of a beam deflection due to constant static loads, one can obtain integrals which often do not have exact solutions or these solutions are described by long equations. In this case, a numerical integration is advantageous – it can be applied for multi-segment bars having shapes described by various functions (cf. e.g. Chalecki, Jaworski, Szlachetka & Bagdasaryan, 2018).

The paper is aimed on presentation of application of such approach in calculations of first natural frequency of multi-segment simply supported beams, symmetrical with respect to their midpoint, having a constant width and variable height. It has been considered a beam consisting generally of five segments (Fig. 1a). Moreover, it has been assumed that the vibration amplitude is small, the material is homogeneous, isotropic and ideally elastic, the bars are slender and the mass is distributed uniformly over the whole bar. The Mathematica software was employed to the calculations. The results were compared to those obtained with FEM software (ANSYS) and for some cases – to the literature data.

Algorithm of proceeding

As the beam depicted in Figure 1a is symmetrical with respect to its midpoint, its natural frequency is the same as for the "halved" beam – sliding in the cut point. Its scheme is shown in Figure 1b.

Cross section area $A(x)$ and second area moment $J(x)$ depend on the beam height $\eta(x)$, thus for consecutive segments are equal to, respectively:

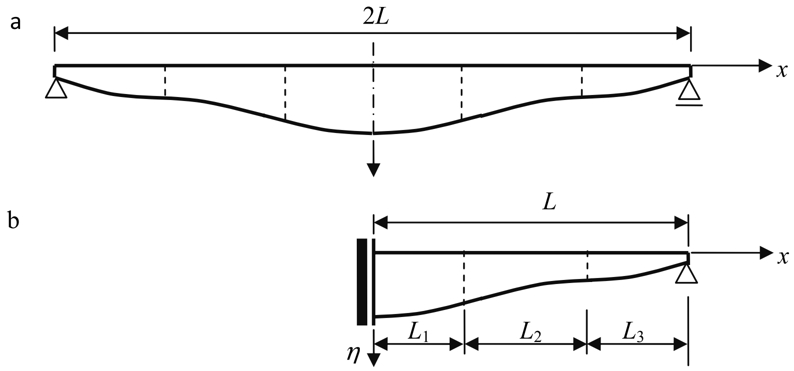

FIGURE 1. General scheme of beams under consideration (a); equivalent beam with lengths of individual segments (b)

Cross section area $A(x)$ and second area moment $J(x)$ depend on the beam height $\eta(x)$, thus for consecutive segments are equal to, respectively:

$$A^{(j)}(x) = b\eta^{(j)}(x),$$
$$J^{(j)}(x) = \frac{1}{12} b\left(\eta^{(j)}(x)\right)^3, \tag{1}$$

where:
b – constant width of the cross section;
j – number of a beam segment ($j = 1, 2, 3$).

Following Jaworski et al. (2015), the beam was loaded by a uniform distributed force. The resulting beam deflection is described by the following second order differential equation of bar elastic deflection curve:

$$EJ(x)\frac{d^2w(x)}{dx^2} = -M_b(x), \tag{2}$$

where:
E – longitudinal modulus of elasticity;
$w(x)$ – deflection;
M_b – bending moment in a cross section given by a coordinate x.

This equation can be solved with Mathematica software.

The assumption that the neutral axis of a bar deflecting due to the vibrations has a shape described by a function $w(x)$ enables to calculate the potential energy for the largest deflection and the kinetic energy in the position of equilibrium. The potential energy E_p and kinetic energy E_k are equal to, respectively:

$$E_p = \int_0^L \frac{1}{2} q w(x) dx, \; E_k = \int_0^L \frac{1}{2} \rho A(x) \omega^2 w^2(x) dx, \tag{3}$$

where:
q – continuous load;
ρ – mass density;
ω – natural frequency;

The energy comparison enables to determine the frequency.

The integrands in formula (3) are very complex, thus the integration has been replaced by summation. In this aim, the first, second and third segment of the beam has been divided into n_1, n_2 and n_3 elements, respectively (Fig. 2), wherein each element has constant height (equal to a relevant height in the element midpoint) and the same length: $l_1 = \frac{L_1}{n_1}$, $l_2 = \frac{L_2}{n_2}$, $l_3 = \frac{L_3}{n_3}$, wherein L_1, L_2, L_3 – lengths of relevant segments. The number of components of the abovementioned summation (quantities n_1, n_2, n_3) must be continuously increased in subsequent iterations. One such iteration encompasses formulas (4)–(14). The summation concerns global deflections of midpoints of each element. Assuming a general shape of the beam shown in Figure 1b, one must execute the following steps to calculate these deflections for a three-segment beam (in the formulas (4)–(13) i_1, i_2, i_3 – integer numbers, $i_1 \in \langle 1, n_1 \rangle$, $i_2 \in \langle 1, n_2 \rangle$, $i_3 \in \langle 1, n_3 \rangle$; for a two-segment beam, relevant terms must be omitted).

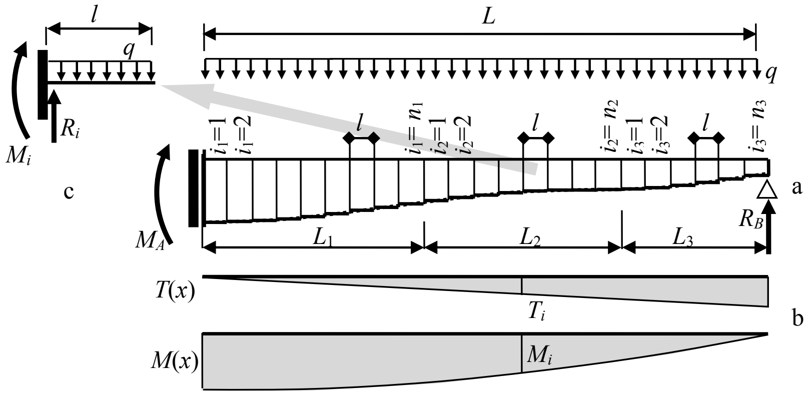

FIGURE 2. Beam discretization (a); diagrams of internal forces (b) and model for calculation of deflections of any individual element (c)

1. Calculation of reaction forces in the left end of each element

This force is equal to an ordinate of the shear force diagram (Fig. 2b). The variability of shear forces is described by the equation $T(x) = -qx$. Considering a reaction for an i-th element ($i = i_1, i_2, i_3$), one must discretize this equation by replacing the variable x by the sum of the lengths of all elements from the first one to that having the number $i - 1$, thus

$$R_{i1}^{(1)} = -qL_1 \frac{i_1 - 1}{n_1},\ R_{i2}^{(2)} = -qL_1 - qL_2 \frac{i_2 - 1}{n_2},\ R_{i3}^{(3)} = -q(L_1 + L_2) - qL_3 \frac{i_3 - 1}{n_3}. \tag{4}$$

2. Calculation of clamp moments in the left end of each element

This moment is equal to an ordinate of the moment diagram (Fig. 2b). The bending moment is described by a quadratic function $M(x) = M_A - \frac{1}{2}qx^2 = \frac{1}{2}qL^2 - \frac{1}{2}qx^2$. Considering a moment for an i-th element ($i = i_1, i_2, i_3$), one must discretize this equation by replacing the variable x by the sum of the lengths of all elements from the first one to that having the number $i - 1$, thus

$$M_{i1}^{(1)} = \frac{1}{2}q(L_1 + L_2 + L_3)^2 - \frac{1}{2}q\left(L_1 \frac{i_1 - 1}{n_1} \right)^2,$$

$$M_{i2}^{(2)} = \frac{1}{2}q(L_1 + L_2 + L_3)^2 - \frac{1}{2}q\left(L_1 + L_2 \frac{i_2 - 1}{n_2} \right)^2, \tag{5}$$

$$M_{i3}^{(3)} = \frac{1}{2}q(L_1 + L_2 + L_3)^2 - \frac{1}{2}q\left(L_1 + L_2 + L_3 \frac{i_3 - 1}{n_3} \right)^2.$$

3. Calculation of deflections of right ends of each element in local coordinates

Each element is treated as a cantilever clamped in the left end and loaded by a uniform distributed force q (Fig. 2c). This force evokes a clockwise reaction moment $M_{ij}^{(i)}$ and upward reaction force $R_{ij}^{(i)}$ (its sense corresponds to the signs „–", appearing in formulas (5)). The deflection of such cantilever is equal to

$$u_{ij}^{(j)} = \frac{1}{EJ^{(j)}} \left(-\frac{1}{2} M_{ij}^{(i)} \left(\frac{L_j}{n_j} \right)^2 - \frac{1}{6} R_{ij}^{(i)} \left(\frac{L_j}{n_j} \right)^3 + \frac{1}{24} q \left(\frac{L_j}{n_j} \right)^4 \right),\ j = 1, 2, 3. \tag{6}$$

4. Calculation of deflections of midpoints of each element in local coordinates

$$\hat{u}_{ij}^{(j)} = \frac{1}{EJ^{(j)}} \left(-\frac{1}{2} M_{ij}^{(i)} \left(\frac{L_j}{2n_j} \right)^2 - \frac{1}{6} R_{ij}^{(i)} \left(\frac{L_j}{2n_j} \right)^3 + \frac{1}{24} q \left(\frac{L_j}{2n_j} \right)^4 \right),\ j = 1, 2, 3. \tag{7}$$

5. Calculation of slopes of right ends of each element in local coordinates

$$\varphi_{ij}^{(j)} = \frac{1}{EJ^{(j)}}\left(-M_{ij}^{(i)}\frac{L_j}{2n_j} - \frac{1}{2}R_{ij}^{(i)}\left(\frac{Lj}{2n_j}\right)^2 + \frac{1}{6}q\left(\frac{L_j}{2n_j}\right)^3\right), j = 1, 2, 3. \tag{8}$$

6. Calculation of deflections of midpoints of each element in global coordinates

The deflection line of the beam from Figures 1b and 2 has the same shape as a deflection line of a cantilever clamped in the left end and loaded with a continuous force q on the whole length and an upward concentrated force in the right end, equal to $q(L_1 + L_2 + L_3)$ – Figure 3, hence at first a way of calculation of deflection U in global coordinates for that very cantilever will be provided.

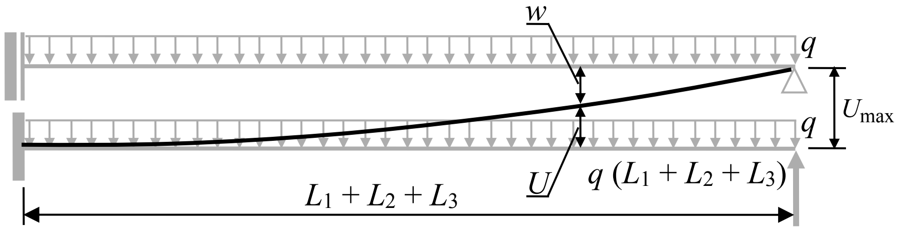

FIGURE 3. Scheme for derivation of formulas for deflections of midpoints in global coordinates

Figure 4 presents a summation scheme for deflections and slopes needed for the calculation of the midpoint deflection of the element i_1 of the first segment (L_1) of the cantilever bar.

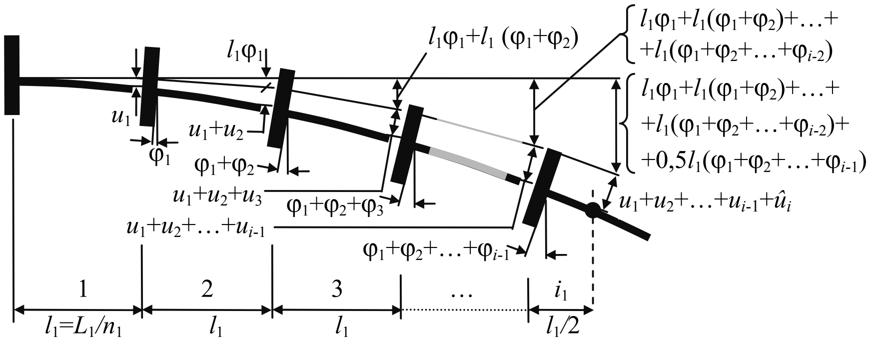

FIGURE 4. Calculation of midpoint deflection of the element i_1 of the first segment of the cantilever bar

According to such scheme, the midpoint deflection of such element is equal to:

$$U_{i1}^{(1)} = \sum_{k=1}^{i_1-1} u_k^{(1)} + \hat{u}_i^{(1)} + \sum_{k=1}^{i_1-1} \varphi_k^{(1)}(i_1 - k - 0.5)\frac{L_1}{n_1}. \tag{9}$$

For the second and third segment the expression for the deflection is derived in analogical way but one has to consider additionally the deflection and slope of the end of the previous segment (Fig. 5). For the elements of the second segment, the deflection of the previous segment (the first one) is equal to $U_{n1}^{(1)} = U_{i1}^{(1)}\Big|_{i_1=n_1}$. Moreover, the deflection resulting from the slope of the midpoint of the last element of the previous segment is equal to:

$$U_{rot1}^{(2)} = \frac{L_1}{2n_1}\sum_{k=1}^{n_1}\varphi_k^{(1)} + \frac{L_2}{n_2}\left(i_2 - \frac{1}{2}\right)\sum_{k=1}^{n_1}\varphi_k^{(1)}.$$

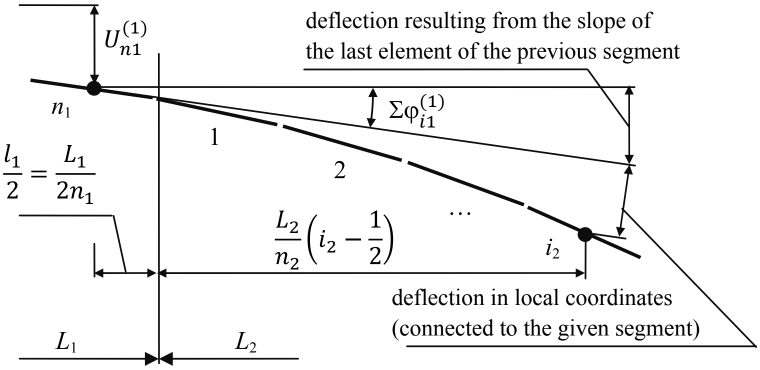

FIGURE 5. Calculation of midpoint deflection of the elements of further segments of the cantilever bar

Thus, the midpoint deflection of the element i_2 of the second segment of the cantilever bar is equal to:

$$U_{i2}^{(2)} = U_{i1}^{(1)}\Big|_{i_1=n_1} + \left[\frac{L_1}{2n_1} + \frac{L_2}{n_2}\left(i_2 - \frac{1}{2}\right)\right]\sum_{k=1}^{n_1}\varphi_k^{(1)} + \sum_{k=1}^{i_2-1}u_k^{(2)} + \hat{u}_i^{(2)} + \\ + \sum_{k=1}^{i_2-1}\varphi_k^{(2)}(i_2 - k - 0.5)\frac{L_2}{n_2}. \tag{10}$$

In a similar way, the deflections and slopes of the previous segments must be considered for the calculation of the midpoint deflection of the element i_3 of the third segment:

$$U_{i3}^{(3)} = U_{i2}^{(2)}\Big|_{i_2=n_2} + \left[\frac{L_2}{2n_2} + \frac{L_3}{n_3}\left(i_3 - \frac{1}{2}\right)\right]\left(\sum_{k=1}^{n_1}\varphi_k^{(1)} + \sum_{k=1}^{n_2}\varphi_k^{(2)}\right) + \sum_{k=1}^{i_3-1}u_k^{(3)} + \hat{u}_i^{(3)} + \\ + \sum_{k=1}^{i_3-1}\varphi_k^{(3)}(i_3 - k - 0.5)\frac{L_3}{n_3}. \tag{11}$$

Now, the appropriate midpoint deflections w of the beam elements can be calculated – according to Figure 3:

$$w_{i1}^{(1)} = U_{i3}^{(3)}\Big|_{i_3=n_3} - U_{i1}^{(1)},\ w_{i2}^{(2)} = U_{i3}^{(3)}\Big|_{i_3=n_3} - U_{i2}^{(2)},\ w_{ij}^{(j)} = U_{i3}^{(3)}\Big|_{i_3=n_3} - U_{ij}^{(j)}, \tag{12}$$

where $U_{i3}^{(3)}\Big|_{i_3=n_3} = U_{\max}$.

7. Energies

Having obtained these deflections, one can replace the integration in (3) by a following summation:

$$E_p = \frac{ql}{2}\left[\sum_{k=1}^{n_1} w_k^{(1)} + \sum_{k=1}^{n_2} w_k^{(2)} + \sum_{k=1}^{n_3} w_k^{(3)}\right],$$

$$E_k = \frac{\rho\omega^2 l}{2}\left[\sum_{k=1}^{n_1} A_k^{(1)}\left(w_k^{(1)}\right)^2 + \sum_{k=1}^{n_2} A_k^{(2)}\left(w_k^{(2)}\right)^2 + \sum_{k=1}^{n_3} A_k^{(3)}\left(w_k^{(3)}\right)^2\right]. \tag{13}$$

8. First natural frequency/period

Comparison of the energies (13) – according to the Rayleigh's method – yields in the first natural frequency and period as a function of deflection w:

$$T = \frac{2\pi}{\omega} = 2\pi\sqrt{\frac{\rho}{q}}\sqrt{\frac{\sum_{k=1}^{n_1} A_k^{(1)}\left(w_k^{(1)}\right)^2 + \sum_{k=1}^{n_2} A_k^{(2)}\left(w_k^{(2)}\right)^2 + \sum_{k=1}^{n_3} A_k^{(3)}\left(w_k^{(3)}\right)^2}{\sum_{k=1}^{n_1} w_k^{(1)} + \sum_{k=1}^{n_2} w_k^{(2)} + \sum_{k=1}^{n_3} w_k^{(3)}}}. \tag{14}$$

The deflection includes the quantities q and E, thus q is being reduced and one obtains the period depending on the parameters ρ and E as well as the beam shape.

This is the end of one iteration. Such iterations must be executed so many times till the relative difference between the results of two last iterations T falls under a certain value chosen by a user (e.g. 0.001%). Due to the accuracy of the results being obtained, it is very advantageous to assume a constant length $l = l_1 = l_2 = l_3$, what means that the quantities n_1, n_2 and n_3 should fulfill a proportion $\frac{L_1}{n_1} = \frac{L_2}{n_2} = \frac{L_3}{n_3}$.

Computational examples, accuracy and comparison of results

Two kinds of beams have been investigated: a beam consisting of five rectilinear segments, out of which two have a linearly variable height and the remaining ones – a constant height (cf. Fig. 6a), and a beam consisting of three segments, out of which one has the shape of a parabola convex with respect to the beam axis and the remaining two have a constant height (cf. Fig. 6b). All beams have constant width. The schemes of such beams contain also the most important geometrical parameters. Such beams are widely applied in building construction – they can play a role of floor joists or spans of pedestrian bridges. In both of these cases, the natural frequency is important because it determines the comfort conditions for people and it is necessary to check a serviceability limit state.

For each beam, its height $\eta(x)$ in individual segments was determined and calculations for the beams from Figure 6 were performed; the results are presented in Tables 1–3.

TABLE 1. Values of t for the beam from Figure 6a, $L_1 + L_2 = 0.5L$

L_1	h									
	$0.9H$	$0.8H$	$0.7H$	$0.6H$	$0.5H$	$0.4H$	$0.3H$	$0.2H$	$0.15H$	$0.1H$
0	8.8474	8.9030	8.9757	9.0655	9.1895	9.3563	9.6000	9.9934	10.3141	10.7760
$0.1(L_1+L_2)$	8.8523	8.9184	8.9959	9.1254	9.2836	9.5145	9.8951	10.6306	11.3789	12.9996
$0.2(L_1+L_2)$	8.8573	8.9372	9.0398	9.1895	9.4033	9.7369	10.3526	11.8065	13.5598	17.9728
$0.3(L_1+L_2)$	8.8623	8.9551	9.0897	9.2879	9.5829	10.0832	11.0796	13.6795	17.0021	25.3962
$0.4(L_1+L_2)$	8.8731	8.9785	9.1453	9.4033	9.8053	10.5237	12.0374	16.1212	21.3210	34.2608
$0.5(L_1+L_2)$	8.8881	9.0156	9.2194	9.5402	10.0619	11.0582	13.2048	18.9734	26.2215	43.9933
$0.6(L_1+L_2)$	8.9086	9.0641	9.3349	9.7454	10.4595	11.7894	14.6844	22.3516	31.8276	54.9959
$0.7(L_1+L_2)$	8.9322	9.1232	9.4546	9.9721	10.8957	12.6019	16.2965	25.9350	37.7458	66.3578
$0.8(L_1+L_2)$	8.9536	9.1821	9.5829	10.2201	11.3490	13.4742	18.0027	29.6382	43.7453	77.8906
$0.9(L_1+L_2)$	8.9803	9.2565	9.7326	10.5109	11.8707	14.4492	19.8415	33.5210	50.0399	89.8297
L_1+L_2	9.0056	9.3392	9.8823	10.8059	12.4266	15.4456	21.6931	37.3995	56.3216	101.6106

TABLE 2. Values of t for the beam from Figure 6a, $L_1 + L_2 = L$

L_1		h									
		$0.9H$	$0.8H$	$0.7H$	$0.6H$	$0.5H$	$0.4H$	$0.3H$	$0.2H$	$0.15H$	$0.1H$
0	paper	9.0826	9.4076	9.7925	10.2586	10.8316	11.5713	12.5805	14.0900	15.2104	16.8396
	theory	–	–	9.8108	10.2852	10.8649	11.6120	12.6316	14.1592	15.2956	16.9501
$0.1(L_1+L_2)$		9.1168	9.4888	9.9378	10.4937	11.2121	12.1957	13.6624	16.2538	18.6698	23.4677
$0.2(L_1+L_2)$		9.1467	9.5744	10.1089	10.7931	11.7210	13.0637	15.2702	19.8073	24.6907	35.7531
$0.3(L_1+L_2)$		9.2109	9.7155	10.3569	11.2079	12.4095	14.2482	17.4596	24.5795	32.6486	51.4040
$0.4(L_1+L_2)$		9.2579	9.8480	10.6178	11.6654	13.1835	15.5824	19.9099	29.7793	41.1240	67.6278
$0.5(L_1+L_2)$		9.2921	9.9806	10.8872	12.1444	13.9959	16.9636	22.3901	34.8594	49.2188	82.7398
$0.6(L_1+L_2)$		9.4119	10.2072	11.2763	12.7644	14.9624	18.5073	24.9985	39.8968	57.0058	96.8940
$0.7(L_1+L_2)$		9.5102	10.4211	11.6440	13.3417	15.8561	19.8842	27.2093	43.8822	62.9069	107.0071
$0.8(L_1+L_2)$		9.5872	10.6092	11.9690	13.8505	16.6044	20.9704	28.8001	46.3110	66.0242	111.1978
$0.9(L_1+L_2)$		9.6898	10.8230	12.3026	14.3252	17.2373	21.7529	29.6639	46.7686	65.4555	107.1183
L_1+L_2	paper	9.7839	11.0069	12.5805	14.6758	17.6093	22.0138	29.3517	44.0275	58.7034	88.3117
	theory	9.8014	11.0266	12.6018	14.7021	17.6425	22.0532	29.4042	44.1063	58.8084	88.2126

TABLE 3. Values of t for the beam from Figure 6b

L_1	h									
	0.9H	0.8H	0.7H	0.6H	0.5H	0.4H	0.3H	0.2H	0.15H	0.1H
0	8.8584	8.9958	9.1554	9.3418	9.5716	9.8560	10.2287	10.7579	11.1312	11.6470
0.1L	8.8924	9.1127	9.3316	9.6056	9.9963	10.5031	11.3036	12.9013	14.6348	18.7287
0.2L	8.9393	9.2179	9.4824	9.8883	10.5353	11.4494	13.1147	17.0702	21.8511	33.5366
0.3L	9.0018	9.3552	9.7870	10.2929	11.3427	12.8614	15.7763	22.9049	31.4921	52.1575
0.4L	9.0679	9.4935	10.0785	10.8230	12.3075	14.5307	18.8265	29.2489	41.6527	71.2175
0.5L	9.1569	9.6964	10.4377	11.5326	13.3526	16.2837	21.9084	35.3695	51.2268	88.7775
0.6L	9.2555	9.9440	10.9056	12.3063	14.5569	18.1910	25.0743	41.3360	60.3471	105.182
0.7L	9.3537	10.2013	11.4012	13.0726	15.6620	19.8629	27.6988	45.9401	67.0708	116.610
0.8L	9.4835	10.4588	11.8271	13.6672	16.5726	21.1375	29.4877	48.5351	70.2883	120.749
0.9L	9.6304	10.7309	12.2268	14.2646	17.2798	21.9553	30.2482	48.4885	68.7139	114.458
L	9.7839	11.0069	12.5805	14.6758	17.6093	22.0138	29.3517	44.0275	58.7034	88.3117

The vibration period of a beam depicted in Figure 6 can be expressed as: $T = t\dfrac{L^2\sqrt{\rho/E}}{H}$, where t is a value from Tables 1–3. For the beam of the constant height equal to h, one obtains from the presented procedure $t \approx \dfrac{8.8047}{\frac{h}{H}}$. It is known from the theory (e.g. cf. Rao, 2011) that the first natural frequency of a sliding-pinned beam of the length L is equal to: $\omega = \pi^2\sqrt{\dfrac{EJ}{m(2L)^3}}$. Hence, putting for a rectangular cross-section: $J = \dfrac{bh^3}{12}$, $m = \rho bh \cdot 2L$, it is easy to count: $T = \dfrac{2\pi}{\omega} = \dfrac{8\sqrt{12}L^2}{\pi\left(\frac{h}{H}\right)H}\sqrt{\dfrac{\rho}{E}} \Rightarrow t = \dfrac{8\sqrt{12}}{\pi\left(\frac{h}{H}\right)} \approx \dfrac{8.8213}{\frac{h}{H}}$. The corresponding values are given in two lower grey rows in Table 2. The error is below 0.2%.

Naguleswaran (1994) provided the results for beams tapered linearly from one end to another ($l_1 = 0$, $l_2 = L$ – special case for the beam from Fig. 6a). Basing on them, one can write: $t = \dfrac{2\pi\sqrt{12}}{k} = \dfrac{21.7656}{k}$, where k is a coefficient equal to:

h	0.9H	0.8H	0.7H	0.6H	0.5H	0.4H	0.3H	0.2H	0.15H	0.1H
k	not provided		2.2196	2.1162	2.0033	1.8744	1.7231	1.5372	1.4230	1.2841

The values calculated theoretically with use of this coefficient and the corresponding values obtained with use of the procedure presented above are given in two upper grey rows in Table 2. The percentage differences between these values for the given h vary from 0.19% for $h = 0.7H$ to 0.66% for $h = 0.1H$.

To validate obtained results, the authors used FEM (ANSYS) to test the beams shaped as in Figure 6. For the FEM calculations, the plane stress with thickness element was used. It was assumed: length $L = 10$ m, height $H = 0.8$ m, material – ferroconcrete ($\rho = 2{,}500$ kg·m^{-3}, $E = 40{,}000$ MPa). According to Figure 6, the periods calculated with FEM are generally slightly longer than those obtained with use of the presented method – differences are lower than 0.7% for the beams from Figure 6a and 1.25% for the beams from Figure 6b.

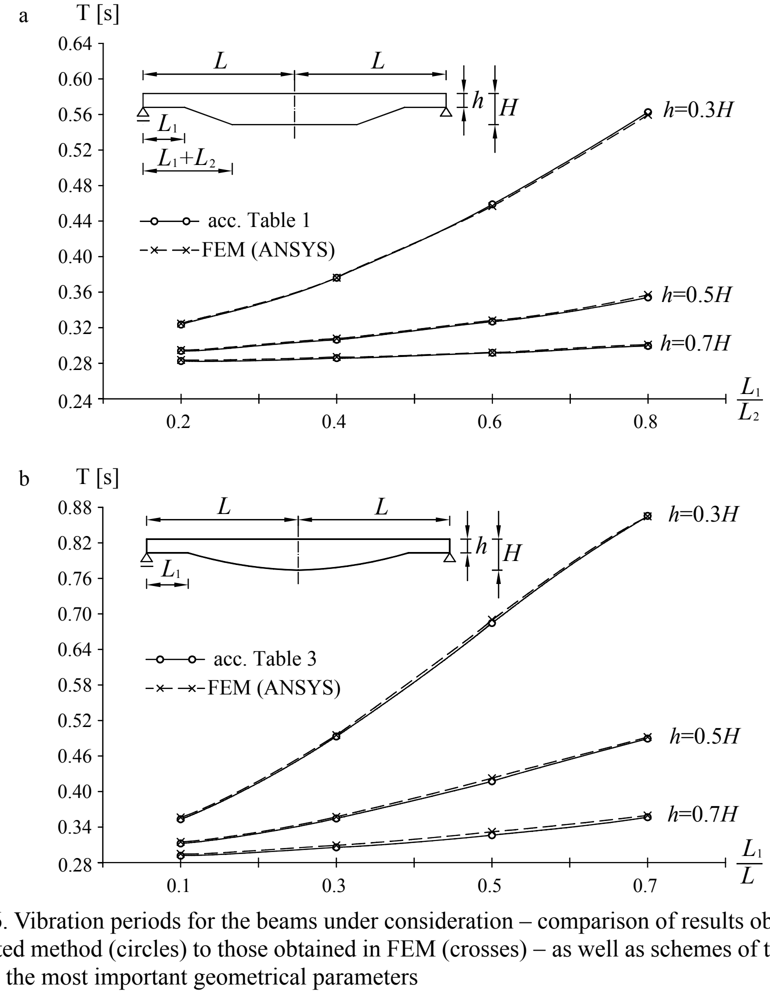

FIGURE 6. Vibration periods for the beams under consideration – comparison of results obtained with the presented method (circles) to those obtained in FEM (crosses) – as well as schemes of those beams along with the most important geometrical parameters

Conclusions

The paper presents a certain procedure of calculation of first natural frequency of three-segment simply supported beams. It has been shown that for approximated calculations of this frequency the Rayleigh's method can be applied – with assumption that the shape of the bar axis deflected during vibration is the same as a shape of the axis of a beam deflected by a uniform continuous static load. The accuracy of this procedure is sufficient for engineering calculations. The procedure can be easily extended to multi-segmented beams by addition of appropriate components. As it is apparent from Figure 3, it can be also applied for cantilever bars.

Replacement of a symbolic integration by the presented procedure (summation) allows considerable simplification of calculations. It can be stated that it often enables to carry out calculations because, in many cases, the symbolic integration is unfeasible even for computers. The procedure is quite simple but exact what can be acknowledged its greatest advantage. The differences between the results obtained in FEM and with use of the procedure do not exceed 1.25%, what is an excellent accuracy from an engineering viewpoint.

Acknowledgements

The authors would like to express their sincere thanks to Jan Grudziński, DEng., for his help in the FEM calculations in the ANSYS.

References

Chalecki, M., Jaworski, J., Szlachetka, O. & Bagdasaryan, V. (2018). Free vibrations of cantilevers – hollow or massive two-part solids of revolution. Resursoekonomnimateriały, Konstrukciji, Budiwli ta Sporudy, Wyp, *36*, 313-320.

Conway, H.D. & Dubil, J.F. (1965). Vibration Frequencies of Truncated-Cone and Wedge Beams. *Journal of Applied Mechanics*, *32*(4), 932-934.

Duan, G. & Wang, X. (2013). Free vibration analysis of multiple stepped beams by the discrete singular convolution. *Applied Mathematics and Computation*, *219*(24), 11096-11109.

Ece, M.C., Aydogdu, M. & Taskin, V. (2007). Vibration of variable cross-section beam. *Mechanics Research Communications*, *34*(1), 78-84.

Jaworski, J. & Szlachetka, O. (2017). Free vibrations of cantilever bars with linear and nonlinear variable cross-section. *Discontinuity, Nonlinearity, and Complexity*, *6*(4), 489-501.

Jaworski, J., Szlachetka, O. & Aguilera-Cortés, L.A. (2015). Application of Rayleigh's method to calculation of the first natural frequency of cantilever columns with variable cross-section. *Journal of Civil Engineering, Environment and Architecture*, *62*(3), 185-194.

Laura, P.A.A., Gutierrez, R.H. & Rossi, R.E. (1996). Free vibrations of beams of bilinearly varying thickness. *Ocean Engineering*, *23*(1), 1-6.

Mao, Q. (2011). Free vibration analysis of multiple-stepped beams by using Adomian decomposition method. *Mathematical and Computer Modelling*, *54*(1-2), 756-764.

Naguleswaran, S. (1994). A direct solution for the transverse vibration of Euler-Bernoulli wedge and cone beams. *Journal of Sound and Vibration*, *172*(3), 289-304.

Naguleswaran, S. (2002). Vibration of an Euler–Bernoulli beam on elastic end supports and with up to three step changes in cross-section. *International Journal of Mechanical Sciences*, *44*(12), 2541--2555.

Naguleswaran, S. (2004). Vibration of an Euler-Bernoulli stepped beam carrying a non-symmetrical rigid body at the step. *Journal of Sound and Vibration*, *271*, 1121-1132.

Rao, S.S. (2011). *Mechanical vibrations*. Upper Saddle River: Prentice Hall.

Szlachetka, O., Jaworski, J. & Chalecki, M. (2017). Analysis of free vibrations of cantilever bars with parabolically variable cross-sections using the Rayleigh's method. *Acta Scientiarum Polonorum. Architectura*, *16*(4), 5-14.

Tan, G., Wang, W. & Jiao, Y. (2016). Flexural free vibrations of multistep nonuniform beams. *Mathematical Problems in Engineering*, 7314280. http://dx.doi.org/10.1155/2016/7314280

Vaz, J.D.C. & de Lima Junior, J.J. (2016). Vibration analysis of Euler-Bernoulli beams in multiple steps and different shapes of cross section. *Journal of Vibration and Control*, *22*(1), 193-204.

Summary

First natural frequency of multi-segment floor joists with variable cross section. The Rayleigh's method can be used to determine the first natural frequency of beams with variable cross-section. The authors analyse multi-segment simply supported beams, symmetrical with respect to their midpoint, having a constant width and variable height. The beams consist generally of five segments. It has been assumed that the neutral bar axis deflected during vibrations has a shape of a beam deflected by a static uniform load. The calculations were made in Mathematica environment and their results are very close to those obtained with FEM.

Authors' address:
Marek Chalecki
(https://orcid.org/0000-0003-3451-458X)
Szkoła Główna Gospodarstwa Wiejskiego w Warszawie
Instytut Inżynierii Lądowej
Wydział Budownictwa i Inżynierii Środowiska
ul. Nowoursynowska 159, 02-776 Warszawa
Poland
e-mail: marek_chalecki@sggw.pl